Lunar Core and Mantle. What Does LLR See?

James G. Williams, Dale H. Boggs

Jet Propulsion Laboratory, California Institute of Technology, Pasadena CA, 91109, USA

James.G.Williams@jpl.nasa.gov

Abstract

The lunar interior is hidden, but Lunar Laser Ranging (LLR) senses interior properties through physical librations and tides. The mean density of the Moon is like rock and the mean moment of inertia is only 1.6% less than a uniform body would have. Neither is compatible with a large dense core like the Earth's, though a small dense core is permitted. The solid-body tides are proportional to Love numbers that depend on interior structure and the radial dependence of elastic parameters and density. A small core, either solid or fluid, increases the Love numbers by a few percent, but uncertainty of deep elastic parameters also affects Love number computations. LLR sees three effects through the physical librations that indicate a fluid core. The strongest effect is from energy dissipation arising at the fluid-core/solid-mantle boundary (CMB). Since there is also dissipation from tides in the solid mantle, we separate tide and CMB dissipation by determining phase shifts in multiple periodic libration terms. The second indicator of a fluid core comes from the oblateness of the CMB which causes a torque as the fluid moves along the oblate surface. The third effect comes from the moment of inertia of the fluid core which affects the amplitude of a physical libration term. The fluid moment is difficult to detect, but it is now weakly seen and its determination should improve from future LLR data. LLR does not separate fluid core density and size, but if the fluid core has the density of iron then a radius of roughly 330-400 km is suggested. Lower density materials would have larger radii; Fe-FeS mixtures are attractive because they have lower freezing points. The dissipation analysis which gives CMB dissipation also gives tidal Q vs frequency. At one month Q is ~30, while Q is ~35 at one year. These low values may come from the lower mantle which is suspected to be a partial melt. How can the core and mantle parameter determinations be improved? Expanded modeling may improve fits and add parameters. Long LLR data spans are important, so future accurate ranges to the four retroreflector arrays are requested. Expanding the number and spread of lunar retroreflector sites, by finding the lost Lunokhod 1 rover or placing new retroreflectors on the Moon, would also benefit the extraction of scientific information from LLR data.

Introduction

Where does the Moon fit in solar system science including origin and evolution? The five terrestrial bodies ordered by increasing size are the Moon, Mercury, Mars, Venus and Earth. Thermal evolution depends on size. The Moon is the smallest and most primitive terrestrial body. The crust is still present, but it was subject to many early large impacts that broke up the surface; at the dark mare areas the original crust is covered with lava flows. Beneath the crust the lunar interior is hidden from direct view and our knowledge of it relies on a variety of evidence. The Moon is an end member in our solar system sample of terrestrial bodies and understanding it contributes to the larger problem of the origin and evolution of the solar system.

Lunar Laser Ranging (LLR) contributes to several scientific areas: lunar science, gravitational physics, geophysics and geodesy, ephemerides and astronomical constants (Dickey et al., 1994). LLR has made significant contributions to lunar science including the lunar interior. The interiors of the planets and satellites are hidden from sight and information on interior structure and properties is difficult to obtain. The lunar interior structure and properties are the subjects of this paper. This paper first reviews some of the relevant information gathered by other techniques, and then discusses what LLR has learned.

Information from Various Techniques

Knowledge of the lunar interior comes from a variety of techniques. To understand the LLR contribution in the larger context, a selective review of some of these results is given in this section. This is a narrow review omitting some topics and references for brevity. A broader modern review of lunar science, including a chapter on the lunar interior, is given in the book New Views of the Moon (Jolliff et al., 2006).

Basic properties of the Moon include mass and radius and the derived mean density. Orbiting spacecraft determine lunar GM (Konopliv et al., 1998), the product of the gravitational constant and the mass. Tracking distant spacecraft also gives the lunar GM since the displacement of the center of the Earth from the Earth-Moon center of mass gives sensitivity. A recent value from DE421 (Williams, Boggs, and Folkner, 2008; Folkner, Williams, and Boggs, 2008) depends most strongly on interplanetary tracking of spacecraft from Earth.

$$GM_{moon} = 4902.80008 \pm 0.00010 \text{ km}^3/\text{sec}^2$$

Dividing GM by the gravitational constant G gives the mass

$$M_{moon} = 7.3459 \pm 0.0011 \times 10^{22} \text{ kg},$$

with the uncertainty in the mass dominated by the uncertainty in G.

From Moon orbiting spacecraft, both laser altimetry and overlapping images have been used to determine lunar topography and the mean radius. The Clementine mission laser altimetry gave a mean radius R of 1737.10 km (Smith et al., 1997). Recent Change'E-1 altimetry gets a mean radius of 1737.01 km (Ping et al., 2008). The recent Kaguya (SELENE) mean radius is 1737.15 km (Araki et al., 2009). With a 1737.1 km radius and the above mass, the mean density is

$$\rho = 3346 \text{ kg/m}^3.$$

This mean density is like rock so any much denser core material must be a small fraction of the total.

Another bulk property of the Moon is the moment of inertia. The three principal moments of inertia around three orthogonal principal axes are A<B<C. The principal axis z near the axis of rotation is associated with moment C while the principal axis x associated with A points near the mean Earth direction. The moments of inertia come from the combination of results from two techniques: orbiting spacecraft gravity field and LLR relative moment differences. From the physical librations, the three-axis rotation or time-variable lunar orientation, LLR determines the moment differences.

$$\beta = \frac{(C-A)}{B} \tag{1}$$

$$\gamma = \frac{(B-A)}{C} \tag{2}$$

The second-degree gravity coefficients are related to the moment differences through their definitions.

$$\frac{(C-A)}{MR^2} = J_2 + 2C_{22} \tag{3}$$

$$\frac{(C-B)}{MR^2} = J_2 - 2C_{22} \tag{4}$$

$$\frac{(B-A)}{MR^2} = 4C_{22} \tag{5}$$

Because we are using the principle axis x to define zero longitude, $S_{22} = 0$. The combination of the LLR and spacecraft results gives the normalized polar moment C/MR^2 and the mean moment I/MR^2. The Konopliv et al. (1998) combination used the R=1738.0 km reference radius that is standard for gravity fields. That radius is close to the mean equatorial radius.

$$C/MR^2 = 0.3932 \pm 0.0002$$
$$I/MR^2 = 0.3931 \pm 0.0002$$

The Clementine, Chang'E-1 and Kaguya mean radii are given above. Rescaling the Konopliv et al. moments to R=1737.1 km gives

$$C/MR^2 = 0.3936 \pm 0.0002$$
$$I/MR^2 = 0.3935 \pm 0.0002$$

The mean value is only 1.6% less than a homogeneous sphere's 0.4. Any increase of density with depth, including the lower density crust and any dense core, will reduce the moment ratios below 0.4, so any dense core must be small.

The detailed structure of the Earth's interior was revealed by seismology. Seismometers were placed on the Moon during the Apollo missions and instruments at four of the sites operated for several years. Two types of moonquakes were detected, shallow and deep moonquakes. The deep moonquakes, from ~750 to ~1100 km deep, were very weak but numerous. Over one hundred source locations are recognized (Nakamura, 2005) and deep moonquakes recur at the same locations, apparently triggered by deep solid-body tides. Impacts were also recognized, both meteoroids and spacecraft. Analysis of the P- and S-wave arrival times by several groups (Goins et al., 1981; Nakamura, 1983; Khan et al., 2000; Lognonné et al., 2003; Gagnepain-Beyneix et al., 2006) showed that the lunar crust was a few tens of kilometers thick and the mantle extended down from the crust through the deep moonquake zone. Deeper structure was not revealed because the damping of the seismic waves became strong below the deep moonquake zone, particularly for the S waves. This attenuating zone is suspected to be a partial melt (Nakamura, 1983). The loss of the S waves prevented deep structure from being determined. There was a second difficulty for lunar seismology; the crust has been broken up by early large impacts and this scatters most of the seismic energy away from the first arrivals of the waves. The damping of seismic waves is very low in the crust and the delayed arrival of scattered seismic waves obscures later arriving waves that

could have been useful. So the Apollo seismic data revealed the lunar crust and mantle, but little is known about the deep-mantle attenuating zone and there is uncertainty about which P waves might have passed through a lunar core (Sellers, 1992). We conclude that the core was undetected or unrecognized by seismology. Lunar seismology is reviewed by Lognonné (2005).

If the Moon had a strong dipole magnetic field it would be persuasive evidence for a liquid core since such fields are considered to arise from dynamos in conducting fluid cores. But there is no strong organized lunar field. The Moon's magnetic field consists of local patches with different polarities. It does not follow that the Moon's core must be solid since sluggish convection in a fluid core may not be vigorous enough to cause a dynamo. It is interesting that many of the basalts brought back from the Mare regions of the Moon are magnetized. This may be evidence for an ancient magnetic field at the time that the Mare flows solidified 3-4 billion years ago (Cisowski et al, 1983; Collinson, 1984; Cisowski and Fuller, 1986), but this explanation is not universally accepted. A 4.2×10^9 year old crustal rock, a troctolite, also shows magnetization so a dynamo could have been active early in the lunar history (Garrick-Bethell et al., 2009).

The Earth's magnetic field deflects the solar wind causing a cavity around the Earth. The Moon lacks a dipole field, so the solar wind impacts and flows around the Moon except when it is passing through the elongated tail of the Earth's cavity. So the Moon is subject to varying external magnetic fields from the solar wind most of the time, but occasionally experiences the quieter field of the geotail. Varying magnetic fields induce currents in the Moon that generate their own magnetic fields that can be sensed by spacecraft magnetometers on or orbiting the Moon. When passing through the geotail these currents decay, with the currents in the most conducting material damping slowest. Apollo-era and more recent Lunar Prospector magnetic data seem to show a long lasting induced field interpreted to be from a conducting core (Goldstein et al., 1976; Russell et al., 1981; Hood et al., 1999). For a core conducting like metals do, the radius inferred by Hood et al. is 340±90 km. For lower conductivity, such as a molten silicate core, the size could be larger.

Rocks brought back from the Moon are highly depleted in minerals involving water and other volatile compounds. The interpretation is that the upper part of the Moon, and perhaps the whole body, was melted when young. During this lunar magma ocean phase, low density materials would have floated to the surface forming the crust. As the Moon cooled the crust and mantle would have solidified. The basalts that make up the dark lunar Mare in low areas came up from partial melts in the upper mantle (Spohn et al., 2001). The basalts are modified mantle material and they have densities higher than the crust. The basalts brought back from the Moon are 3-4 billion years old. The extensive volcanic activity that flooded the dark Mare areas was early in the Moon's lifetime. The mantle convects slowly, radioactive heating is declining and the Moon slowly cools (Spohn et al., 2001). Orbital images show that the cooling Moon produced some lava flows until about 1×10^9 yr ago and there is evidence of very recent gas release (Schultz, Staid, and Pieters, 2006). Heat flow measurements made at two of the Apollo sites help constrain current heat production (Langseth et al., 1976; Warren and Rasmussen, 1987).

Can the core remain molten for the 4.5×10^9 yr age of the Moon? That depends on its composition as well as its initial temperature. A cooling pure iron core would solidify at about 1650° K. However, mixes of iron and other materials have lower melting points, sulfur and carbon are particularly effective. The optimum mixture of iron and sulfur, the eutectic,

stays molten down to ~1000° K (Brett and Bell, 1969). Because the melting point of iron can be lowered so much, Brett (1973) suggested that the lunar core could be molten. A cooling mixture of iron, sulfur and other materials does not solidify at a single temperature. Rather the iron solidifies over a range of decreasing temperatures before the iron-sulfur mixture freezes. This provides a natural way to form a solid iron core interior to the fluid mixture while concentrating the sulfur in the liquid, where it acts like antifreeze.

The liquid or solid state of a core is connected to its temperature and composition. While it is convenient to discuss pure iron as an extreme possibility, iron mixed with sulfur, carbon, nickel, etc are more realistic. It is suggestive that siderophile elements, which would be expected to migrate into a core along with iron, are depleted in lunar rocks when compared to primitive meteorites and the Earth's mantle (Righter and Drake, 1996). As an alternative to iron alloys, dense silicate cores have been proposed. The composition and density of any core should not be considered established.
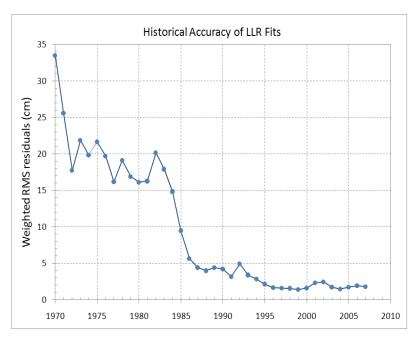
In summary, any dense lunar core must be small to satisfy density and moment of inertia values, and there is magnetic induction evidence that it is conducting. Non-LLR evidence does not establish core composition, though iron alloys are plausible, or whether the core is liquid or solid, or whether there is an inner solid and outer liquid structure. More is known about the mantle. Its density and elastic properties are sampled down to the deep moonquake zone. There may be a partial melt in the deepest part of the mantle above the core.

LLR Evidence

Early LLR lunar science included moment of inertia differences and low-degree gravity field coefficients. Previous reviews are given by Dickey et al. (1994) and Williams and Dickey (2003). At the end of the 1970s LLR found a strong energy dissipation signature, a displacement in the direction of the precessing pole of rotation. It took two decades to separate the two causes, tidal dissipation in the Moon and dissipation at the fluid-core/solid-mantle boundary (CMB). LLR is also sensitive to potential Love number k_2, displacement Love numbers h_2 and l_2, tidal dissipation at several frequencies, flattening of the CMB, and moment of inertia of the fluid core. All of these parameters tell us something about the lunar interior.
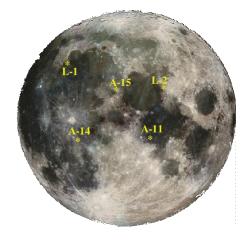
LLR Data, Stations and Retroreflector Arrays

The LLR data analysis uses ranges from 1970-2008. The initial conditions for the lunar ephemeris and three dimensional lunar orientation (Euler angles and spin rates), lunar laser retroreflector array positions, lunar geophysical parameters, and other parameters including Earth orientation and station positions and rates were fit to Lunar Laser Ranging (LLR) data. A total of 16,941 ranges extend from March 16, 1970 to November 22, 2008. Modern range accuracies are more than an order-of-magnitude more accurate than the early data. Ranges were processed from McDonald Observatory, Texas (6,523 ranges), Observatoire de la Côte d'Azur (OCA), France (9,177), Haleakala Observatory, Hawaii (694), Apache Point Observatory, New Mexico (536), and Matera, Italy (11). LLR data are archived by the ILRS (Pearlman et al., 2002). The Apache Point Observatory is a high accuracy addition to the LLR network (Murphy et al., 2009). Figure 1 shows the annual weighted rms range residuals after fits. The weighted rms residual for the past 4 yr combined is 0.11 nsec or 1.67 cm. The Apache Point ranges and the best of the OCA data cannot be fit to their noise levels. Shortening the data span in the fit reduces the rms residual, so there is a long-time signature that is not being fit.
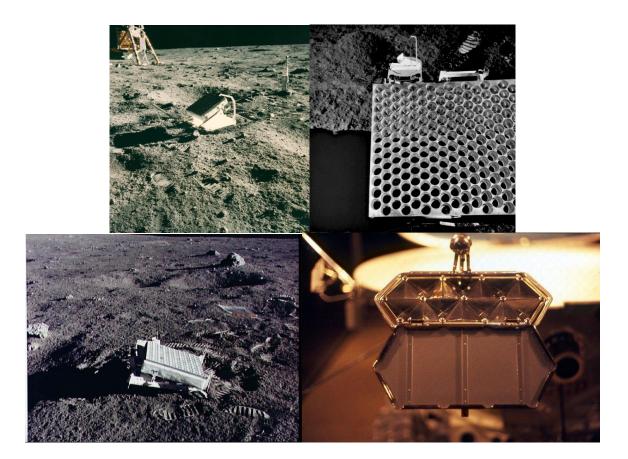
Figure 1. Weighted rms range residuals improve with time.

Ranges to four retroreflector arrays on the Moon are used in fits. Arrays are located at the Apollo 11, 14, 15 and Lunokhod 2 sites shown in Fig. 2. Lunar landing site maps, images and descriptions are presented by Stooke (2007). A majority of the ranges are to the largest array at the Apollo 15 site (77.5%), while Lunokhod 2 gets the fewest number of ranges (2.8%). Apollo 11 and 14 make up 9.9% and 9.7% of the total data set, respectively. The Lunokhod 1 position has not been known well enough to acquire ranges. A proposed location is given by Stooke (2005). Finding and ranging Lunokhod 1 would benefit the tide measurements. The Lunokhod 2 array now gives a weak return (Murphy et al., 2009) and Lunokhod 1 may also be weak and hard to find. The coordinates of known LLR sites are available (Williams, Newhall and Dickey, 1996; Williams, Boggs and Folkner, 2008) and are used for lunar geodesy. Figure 3 shows the four arrays. Ranges to multiple arrays are important for determining the physical librations, tides and lunar geophysical parameters.

Figure 2. Locations of retroreflecting arrays on the Moon.

Figure 3. Retroreflecting arrays on the Moon at the Apollo 11 (upper left), 14 (lower left) and 15 (upper right) sites. The French-built array (lower right) projects out from the front of the Soviet Lunokhod rover.

Physical Librations

Many of the lunar geophysical parameters affect the 3-axis lunar rotation and orientation, the physical librations, and that gives LLR sensitivity to those effects. This sensitivity is illustrated by the equations of motion for the vector rotation of the lunar mantle and fluid core. Those three-dimensional rotations are coupled by two interactions at the core/mantle boundary (CMB).

$$\frac{dI_m\omega_m}{dt} + \omega_m \times I_m\omega_m = T_g + T_{cmb} \tag{6}$$

$$\frac{dI_f\omega_f}{dt} + \omega_m \times I_f\omega_f = -T_{cmb} \tag{7}$$

$$T_{cmb} = K_v(\omega_f - \omega_m) + (C_f - A_f)(\hat{z} \cdot \omega_f)(\hat{z} \times \omega_f) \tag{8}$$

The first differential equation is the Euler equation for the mantle with torques on the right-hand side. The rotating mantle provides the frame with axes aligned with the mean principal axes of the mantle.

- I_m is the mantle moment of inertia matrix including tidal deformation. The mean moment matrix is diagonal with principal moments A_m, B_m and C_m, but the tidal variation matrix is 3x3.
- ω_m is the spin rate vector for the mantle. The spin rate components are functions of the Euler angles and their rates.

- T_g is the gravitational torque vector from the lunar gravity field, degree 2-4, interacting with the Earth, Sun, Venus, Mars, and Jupiter. The degree-2 field is subject to variations due to tides and spin. Also included is the figure-figure torque from degree-2 Earth x degree-2 Moon.
- T_{cmb} is the torque vector from two interactions at the fluid-core/solid-mantle boundary. Since the core and mantle have different spin rate vectors, the fluid moves with respect to the solid mantle and forces arise. The CMB dissipation and oblateness forces are the two interactions. Integrating the local torques over the CMB surface gives the total torque. The unit z vector is the mantle principal axis corresponding to moment C_m.

The second differential equation is written for a uniform fluid core, assumed to be rotating like a solid, but using the frame of the mantle. The mantle frame is used because the mantle controls the CMB shape and the nonspherical moments of inertia of the fluid.

- I_f is the fluid moment of inertia tensor including an oblate CMB. The mean moment matrix is diagonal in the mantle frame with principal moments A_f, A_f and C_f.
- ω_f is the spin vector for the mantle.
- Torque $-T_{cmb}$ now enters with sign reversed from the mantle torque.

The above differential equations show that the rotation of the Moon is sensitive to moments of inertia of mantle and fluid core, lunar gravity field, tidal deformation (Love number k_2 with a time delayed response for dissipation), dissipation at the CMB, and flattening at the CMB. The differential equations for vector rotation and lunar and planetary orbits are integrated numerically.

Fluid Core Moment of Inertia
The fluid core moment of inertia is the latest lunar geophysical parameter to emerge from the LLR analysis. This is a valuable new result. Sensitivity comes because the orientations of both mantle and fluid core follow the slow motion of the ecliptic plane, while the core has diminished response to faster variations (see Sidereal Terms in Williams et al., 2001). The solution for the ratio of fluid moment to total moment gives $C_f/C = (12\pm4)\times10^{-4}$. For a uniform liquid iron core without an inner core this value would correspond to a radius of 390±30 km while for the Fe-FeS eutectic the radius would be 415 km. Those two cases would correspond to fluid cores with 2.4% and 2.2% of the mass, respectively. With a solid inner core, assuming that the inner core orientation is gravitationally coupled to the mantle so that they precess together, the fluid moment depends on the fluid density and outer and inner radii, $(8/15)\pi\rho_f(R_f^5 - R_{ic}^5)$. So the outer (CMB) radius would be larger if there is a solid inner core.

In the past we have inferred the fluid core moment of inertia and radius from LLR dissipation results (Williams et al., 2001). Those inferred moments were about half of the new result. Our 2001 paper used Yoder's boundary layer theory for dissipation at the CMB (Yoder, 1995), but did not keep a factor of ½ in Yoder's expression for torque. That factor would reconcile the two approaches. Otherwise, the dissipation results tend to give an upper limit for fluid core moment because any topography on the CMB surface will increase the dissipative torque. Any inner core would provide a second surface for dissipation so that a smaller CMB radius would account for the dissipative torque.

While the new result for core moment is noisy, any core result that involves size and density is important. The moment uncertainty should improve as the LLR data span increases. The

main difficulty with using this direct approach comes from separating three effects, core moment and two free precessions, causing slow motions of the pole in space (Williams et al., 2001). The increasing LLR data span is improving the separation and reducing the uncertainty.
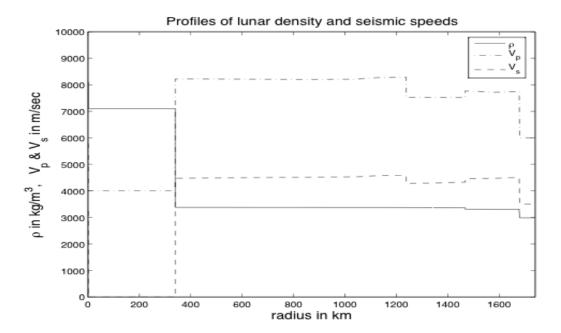
Tides

The elastic response of the Moon to a tide-raising force is given by Love numbers. At the Moon's distance from the Earth, >99% of the size of the tidal response is described by the three second-degree Love numbers. LLR sensitivity to the potential Love number k_2 comes from physical librations. In the above differential equations, our software distorts the mantle moment matrix I_m on the left-hand side while for the gravitational torque T_g on the right-hand side the total moment matrix is distorted (appropriate for a uniform fluid core without an inner core). For the solutions being presented I_f was not distorted in the model, though that refinement is being added to the software. There is a small contribution for spin distortion, but the variation of distortion from spin is small compared to tides. Orbiting spacecraft can determine the lunar Love number k_2 from tidal variation of the gravity field. Results are 0.026±0.003 (Konopliv et al., 2001), 0.0248 in the LP150Q gravity solution (Konopliv, PDS website), and 0.0213±0.0075 (Goossens and Matsumoto, 2008).

While k_2 is a dynamical parameter, the displacement Love numbers h_2 for the vertical tides and l_2 for the horizontal are determined from tidal displacement of the retroreflectors. Tidal variations are about ±0.1 m for vertical and half that for horizontal. If one solves for h_2 and l_2 the correlation is 0.73 and the separation is weakened by an unfavorable distribution of retroreflector X coordinates (toward the mean Earth direction) on the Moon. There is elastic information from the Apollo seismometers, but that information does not extend to the lower mantle and core. Of the three Love numbers, l_2 is least sensitive to the deep zones so we solve for k_2 and h_2 while fixing l_2 at a model value of 0.0105. Solutions give k_2 = 0.0199±0.0025 and h_2 = 0.042±0.008.

Model Love numbers are calculated using seismic P- and S-wave speeds deduced from Apollo seismometry. The seismic speeds have to be extrapolated from the sampled mantle regions into the deeper zone above the core. Figure 4 shows radial profiles for density and seismic speeds. A 340 km liquid iron core was added to a mantle model from Kuskov and Kronrod (1998). The resulting model Love numbers are k_2=0.0225, h_2=0.0394, and l_2=0.0106. Another model with a 390 km radius liquid iron core gives k_2 of 0.0233, h_2 of 0.0408, and l_2 of 0.0107. The Apollo seismic uncertainties contribute several percent uncertainty to the three model Love numbers and the core adds further uncertainty. A larger core increases the model k_2 and h_2 values, but has less effect on l_2. Any partial melt above the core would increase k_2 and h_2.

There are substantial uncertainties, but the k_2 values from LLR as well as Goossens and Matsumoto are more compatible with a smaller core while the Konopliv k_2 values and the LLR h_2 and core moment results favor a larger core. While this apparent conflict is not large compared to uncertainties, it does deserve attention as new results become available. We are exploring whether tidal deformation of the core/mantle boundary will make a significant difference for the LLR k_2 determination.

Figure 4. Lunar density and P- and S-wave speeds vs radius. The liquid iron core radius is 340 km. V_P is greater than V_S, and V_S is zero in the fluid.

Dissipation from Tides and Core

There are many small perturbations on the orientation of the lunar orbit and equator planes, but there is one big effect. The Moon's mean orbit plane is tilted by 5.145˚ to the ecliptic plane and the orbit plane precesses in a retrograde direction along the ecliptic plane with a retrograde 18.6 yr period. The lunar equator also precesses along the ecliptic plane with an 18.6 yr period, but the tilt of 1.543˚ is in the opposite direction from the orbit. So the angle between the orbit and equator is 6.69˚. Without dissipation, the ascending node of the orbit matches the descending node of the lunar equator so that the orbit, ecliptic and rotation poles are coplanar. When the rotation is subject to energy dissipation, either from tides or CMB effects, the rotation pole is shifted slightly in the direction of precession, and the alignment of three planes is no longer exact. Such a displacement of the mean pole of rotation/mean equator was seen three decades ago with the LLR data. While at least some of the displacement had to be due to tidal dissipation, it was not then known if the Moon had a fluid core though that possible explanation was proposed by Yoder (1981).

The key to separating the two causes of dissipation was the detection of small physical libration effects of a few milliarcseconds (mas) size. Guided by semi-analytical theories for tide and core dissipation (Williams et al., 2001), we solve for periodic terms in longitude physical librations at 1 yr (annual mean anomaly), 206 d, and 1095 d (1/2 period of argument of perigee) in addition to a tidal time delay and the fluid core K_v. The tidal time delay and the CMB dissipation are both effective at introducing a phase shift in the precessing pole direction. The three small periodic terms allow for tide-induced phase shifts in physical libration periodicities. Third-degree gravity coefficients also cause phase shifts. We adopt C_{31}, S_{31}, and S_{33} from spacecraft determined LP150Q (Konopliv, website) and use the LLR data to solve for the four remaining third-degree coefficients. The solution gives dissipation from the CMB and tides. Both are strong contributors to the 0.27" offset of the precessing rotation pole from the dissipation-free pole, equivalent to a 10" shift in the node of the equator on the ecliptic plane. There is a weak dependence of tidal specific dissipation Q on

110

period. The Q increases from ~30 at a month to ~35 at one year. Q for rock is expected to have a weak dependence on tidal period, but it is expected to decrease with period rather than increase. The frequency dependence of Q deserves further attention and should be improved.

Core Oblateness

Detection of the oblateness of the fluid-core/solid-mantle boundary (CMB) is independent evidence for the existence of a liquid core. In the first approximation, CMB oblateness influences the tilt of the lunar equator to the ecliptic plane (Dickey et al., 1994). Parameters for CMB flattening, core moment of inertia, and core spin vector, are introduced into torque T_{cmb} in the numerical integration model used for lunar orientation and partial derivatives. Equator tilt is also influenced by moment-of-inertia differences, gravity harmonics and Love number k_2, solution parameters affected by CMB oblateness. Solutions can be made using the core and mantle parameters.

Torque from an oblate CMB shape depends on the product of the fluid core moment of inertia and the CMB flattening, $fC_f=(C_f-A_f)$. Both are uncertain and there is no information about flattening apart from these LLR solutions. The LLR solution gives $f=(C_f-A_f)/C_f=(2.0\pm2.3)\times10^{-4}$. For a 390 km core radius the flattening value would correspond to a difference between equatorial and polar radii of about 80 m with a comparable uncertainty. The f uncertainty seems to imply no detection, but the oblateness parameter f correlates -0.90 with core moment. The derived oblateness varies inversely with fluid core moment, as expected theoretically, so a smaller fluid core corresponds to a larger oblateness value. The product $fC_f/C=(C_f-A_f)/C=(3\pm1)\times10^{-7}$ is better determined than f alone. Core flattening appears to be detected and the foregoing product is more secure in a relative sense than the value of f itself. In the solution of this paper the corrections to core moment and CMB flattening were substantial compared to the prefit DE421 values. In the earlier solution leading to DE421 the fluid core moment was fixed (Williams, Boggs and Folkner, 2008). Updated values are anticipated with the next ephemeris.

The influence of the CMB flattening on the mantle's forced precession depends on the product of the flattening and core moment, as given above. Core oblateness can also cause a retrograde free precession in space of the orientation of the fluid core, which has a small influence on the mantle. In the case of the Earth, this free precession in space is often considered in a frame rotating with the body and it is often called the free core nutation (FCN). The free precession frequency is proportional to the flattening f (Gusev et al., 2005; Petrova and Gusev, 2005). Since the LLR solution shows a large correlation between core moment and flattening, we conclude that the forced term is more important to the LLR solution than the free precession. The fluid core free precession period (1/fn, where n is mean motion) appears to be greater than a century, >170 yr if we use the solution f plus its uncertainty. Small amplitude and long period make the core free precession difficult to distinguish directly from four decades of LLR data.

The Moon's figure is subject to tide and spin distortions. If the mantle supported no shear stresses, like a fluid, then the Moon's figure would be an equilibrium figure for the tides and spin. The model equilibrium value for the CMB flattening is $f_e=2.2\times10^{-5}$. The equilibrium product f_eC_f/C is an order-of-magnitude smaller than the fC_f/C value found by LLR and the latter would require a 3σ discrepancy to agree with the equilibrium value. Thus, the CMB flattening does not appear to be close to equilibrium. For comparison, the whole Moon degree-2 shape (Smith et al., 1997; Araki et al., 2009; Ping et al., 2008), gravity field (Konopliv et al., 1998, 2001) and moment of-inertia differences (Dickey et al., 1994) are an

order-of-magnitude larger than the equilibrium figure expected from the current tides and spin. The same appears to be true for the CMB flattening.

Free Librations
Dissipation has been recognized by LLR from both tidal flexing and the fluid/solid interaction at the core/mantle boundary. Dissipation introduces a phase shift in each periodic component of the forced physical librations. The differential equations for lunar rotation have normal modes, three for the mantle and one for the fluid core. It might be expected that that the free physical librations associated with these normal modes would be imperceptible since the damping times are short compared to the age of the Moon. However, substantial motions are found for two of the modes (Calame, 1976ab; Jin and Li, 1996; Newhall and Williams, 1997; Chapront et al., 1999; Rambaux and Williams, 2009ab) and we have to ask what is the source of stimulation.

Reported here are results from the recent effort with Rambaux that analyzed the DE421 physical librations. The free physical librations depend on the initial conditions for the Euler angles and spin rates, which are adjusted during the LLR fits. The integrated Euler angles were fit with polynomials plus amplitudes and amplitude rates for trigonometric series. More than 130 periodic terms were recognized in two latitude libration angles, while longitude libration yielded 68. The free libration terms were identified among many forced terms.

The longitude mode is a pendulum-like oscillation of the rotation about the (polar) principal axis associated with moment C. The period for this normal mode is 1056 d = 2.89 yr. Recovering the amplitude is complicated by two forced terms very close to the resonance period. A first approximation for the two forced terms results in a free amplitude of 1.3", or 11 m at the equator. From the dissipation results, the damping time is calculated to be 2×10^4 yr using expressions in Williams et al. (2001).

The lunar wobble mode is analogous to the Earth's polar motion Chandler wobble, but the period is much longer and the path is elliptical. Observed from a frame rotating with the lunar crust and mantle, the rotation axis traces out an elliptical path with a 74.6 yr period. The amplitudes are 3.3"x8.2" (28 m x 69 m). The minor axis of the ellipse is toward the mean Earth direction. LLR has followed this elliptical motion through half a cycle. The computed damping time is about 10^6 yr.

The two remaining free modes are retrograde precession modes when viewed from a nonrotating frame in space. The mantle free precession of the equator (or pole) has an 81 yr period. An amplitude of 0.03" is found for this mode, but there is uncertainty because the LLR fit for the integration initial conditions appears to be sensitive to the lunar interior model. The expected damping time is 2×10^5 yr. The fluid core free precession of the fluid spin vector has an expected period >170 yr, as previously discussed under Core Oblateness; it would be 197 yr for the DE421 integration. Based on the trigonometric analysis, this mode must have a small amplitude.

The two free modes with large amplitudes can be stimulated by internal lunar processes, but internal stimulation is an inefficient way to generate the free precession of the mantle. The longitude mode can also be stimulated by resonance passage, as has been proposed by Eckhardt (1993) and confirmed by Newhall and Williams (1997). Yoder (1981) proposed that the free wobble could be generated by fluid eddies formed at the core/mantle boundary.

Uncertain stimulating mechanisms for free librations, including the possible connection to the lunar interior, makes the free librations of continuing interest.

Search for a Solid Inner Core
It is reasonable to expect that the Moon would have a solid core interior to the fluid core, but it remains undetected. The phase diagram for Fe-FeS shows that cooling of fluid alloys of iron and sulfur would freeze out part of the iron while concentrating sulfur compounds in the fluid (Brett and Bell, 1969). There is no direct evidence for a solid inner core. An inner core might be detected through its influence on physical librations or gravity, or through seismology. Any detection would establish the last major unit of the Moon's structure.

Lunar Laser Ranging is sensitive to small effects in the lunar physical librations. Predicting the size of these effects depends on a number of unknown parameters including the inner core moment of inertia and gravity field, and the mantle's gravity field interior to the CMB. An inner core might be rotating independently or it might lock to the mantle rotation through gravitational interaction. The inner core and mantle interact through their nonspherical gravity fields. This gravitational interaction is probably very much stronger than torques from the fluid core so we assume that the mean rotation rates of mantle and inner core are the same. The inner core also interacts gravitationally with the Earth. Like the mantle, the orientation of the inner core is expected to precess at the same node rate as the mantle, but not necessarily with the equator of the inner core exactly aligned with the mantle's equator. The tilts between the two equators and the ecliptic plane will be different and this difference will cause a small variation in the external gravity field of the Moon that might be detected by spacecraft (Williams, 2007). A strong gravitational interaction between inner core and mantle tends to align their equator planes and a very weak interaction makes the orientations more independent. The inner core rotation dynamics has a resonance if the precession normal mode frequency of the inner core matches the forcing frequency of $-1/18.6$ yr. Close to such a resonance the two orientations could be very different. There are other forcing frequencies that can also resonate causing potentially observable effects in the physical librations. The frequency of the precession-like normal mode would determine which physical libration terms would get modified most strongly.

An inner core can also modify the physical librations in longitude. There are a large number of forcing terms for longitude librations. The inner core introduces a new normal mode with a natural frequency and that frequency will determine which longitude libration periodicities are most strongly affected. The period of the normal mode might be from less than one year to decades.

To look for inner core effects, the postfit LLR residuals for each retroreflector array have been analyzed to produce spectra. The Apollo 11 and 14 arrays are near the equator (see Fig. 2), so they will be most sensitive to longitude librations. The Apollo 15 array, well north of the equator with a small longitude, provides the most sensitivity to latitude librations. The Lunokhod 2 array is sensitive to both longitude and latitude librations, but the smallest number of observations (477 is 2.8%) gives this array the noisiest spectra. All of the spectra are highest for periods longer than a year. The Apollo 11 spectrum is highest on either side of the 1056 d mantle resonance: 9 mm at 850 d and 10 mm at 1350 d. The Apollo 14 spectral amplitudes are highest at 1200 d (9 mm) and 2200 days (11 mm). The latter period is very interesting because it coincides with a 2190 d = 6.0 yr argument of perigee period that is a forcing term. The phase aligns more closely with the cosine of argument of perigee. If from longitude librations, the amplitude at 6.0 yr should also show in the Apollo 11 spectrum with

opposite sign from Apollo 14, but we find a 5 mm amplitude with the same sign. So we cannot claim detection of an anomalous libration amplitude at 6.0 yr. The amplitudes for the Apollo 15 spectrum are all <5 mm.

The detection of the Moon's inner core will be a major accomplishment for any technique. For LLR it is a future possibility.

Orbit Evolution

Dissipation in the Moon and Earth causes slow changes in the lunar orbit. The semimajor axis and eccentricity increase with time and the inclination decreases. Dissipation in the Moon also deposits heat in the Moon. This is a minor effect now, but could have been much more important when the Moon was closer to the Earth. Here we summarize the orbit changes.

Table 1 presents dissipation-induced secular rates for mean motion n, eccentricity e, and Earth rotation rate ω. LLR results on two lines are compared with model computations on three. The LLR integration model for terrestrial tidal dissipation uses Love numbers and time delays for three frequency bands: zonal (long period), diurnal, and semidiurnal. For DE421 the three Love numbers and the zonal time delay were set to model values. The diurnal and semidiurnal delays were fit to LLR data in creating DE421. For the Moon, the lunar Love number k_2, time delay, and CMB dissipation parameter K_v were fit for DE421. The Earth and Moon related rates in the table are computed from the DE421 Earth and Moon parameters. For the LLR fits, the Earth tide parameters are sensed through the orbit changes, but the lunar parameters are mainly determined from the physical librations. The anomalous eccentricity rate is not present in the DE421 integration, but a rate of unknown cause is routinely found to be significant. For comparison, model values of dn/dt, de/dt and dω/dt were computed for the Earth based on the IERS Conventions (McCarthy and Petit, 2003) for the main body and FES2004 results for the ocean tides (Lyard et al., 2006; Ray, 2007). There is some uncertainty in converting the terrestrial Love numbers and time delays to orbit rates, but the same theoretical expressions were used for converting the LLR and Earth model parameters and that should minimize differences. The results are presented in Table 1.

Table 1. Dissipation-induced rates for mean motion, eccentricity, and Earth rotation comparing LLR to an Earth model.

	units	zonal	diur-nal	semi-diurnal	Earth sum	lunar tides	lunar CMB	Moon sum	anom-alous	total
LLR dn/dt	"/cent^2	0.12	-3.31	-22.88	-26.07	0.20	0.02	0.22		-25.85
LLR de/dt	10^{-11} /yr	-0.03	0.16	1.20	1.33	-0.40	0	-0.40	1.32	2.25
model dn/dt	"/cent^2	0.12	-3.76	-22.61	-26.25					
model de/dt	10^{-11} /yr	-0.03	0.22	1.54	1.73					
model dω/dt	"/cent^2	0	-196	-1125	-1321					

In the table note that the total Earth dn/dt from LLR and the Earth model differ by <1%. An independent LLR analysis for total dn/dt of –25.858 ”/cent^2 (Chapront et al., 2002) gives very good agreement with the DE421 mean longitude acceleration of –25.85 ”/cent^2 given here. The DE421 value corresponds to a 38.14 mm/yr rate for semimajor axis. There is less agreement between eccentricity rate from LLR and the Earth model because the LLR solutions mainly accommodate the tidal acceleration dn/dt that very strongly affects the LLR data. Most of the Earth tide de/dt comes from the N2 tide, while for dn/dt the M2 and O1 contributions are larger. For the lunar tides, the component with the anomalistic period is most important for de/dt. Accounting for the difference in de/dt from the simple LLR integration model and the more complete Earth model, the unexplained eccentricity rate is $(0.9\pm0.3)\mathrm{x}10^{-11}$ /yr, equivalent to an extra 3.5 mm/yr in the perigee rate. The inclination rate is not given in the table since it is computed to be only $-1\mathrm{x}10^{-6}$ ”/yr. The predicted Earth spin rate change is given in the last line of the table. In decreasing order, the most important tides for secular rotation acceleration are M2, S2, K1, O1, and N2. The S2 and K1 tides do not cause secular changes in lunar mean motion or eccentricity.

There is no evidence for any anomaly in the tidal acceleration in mean longitude. By contrast, the anomalous lunar eccentricity rate indicates that something is not understood well enough. Though it cannot be said with certainty that the anomaly comes from the Moon, the lunar interior is less well known than the Earth's interior. Computation of lunar orbit evolution over long times needs a good understanding of the various contributions to the secular rates. Long-time evolution of the orbit is complex because of evolving lunar thermal conditions and changing ocean tides (Bills and Ray, 1999).

Lunar Ephemeris
Selected lunar and planetary ephemerides are made available for scientific and mission use. The latest recommended lunar and planetary ephemerides and lunar physical librations make up DE421. The DE421 ephemeris may be downloaded in an ascii version from

<p style="text-align:center">ftp://ssd.jpl.nasa.gov/pub/eph/planets/ascii/de421 .</p>

The complete set of input parameters for the solar system integration is part of the file. The SPICE kernel version of DE421 is available at

<p style="text-align:center">ftp://ssd.jpl.nasa.gov/pub/eph/planets/bsp .</p>

Documentation is available in two memos (Williams, Boggs, and Folkner, 2008; Folkner, Williams, and Boggs, 2008).

Conclusions and Future Possibilities

Among the five major terrestrial bodies, the Moon is a primitive end member. Most of the large surface features are ancient, $3\mathrm{x}10^9$ to $4\mathrm{x}10^9$ yr old compared to the $4.5\mathrm{x}10^9$ yr age of the Earth and Moon. At very early times, at least the upper part of the Moon was molten, perhaps all of it was melted. As the Moon cooled, the crust and mantle solidified, volcanism flooded the Mare areas, became infrequent, and ended. Today's Moon is slumbering, but not dead.

The analysis of data from several techniques provides clues about the lunar core and deep interior. The lunar mean density and moment of inertia permit a small dense core, but not a large core. That core could be solid or liquid. Analysis of Apollo-era seismic data provides

information on the elastic properties of crust and mantle and shows that S waves damp out for the deep mantle, possibly due to a deep partial melt. P waves penetrate the deepest mantle better, but the seismic data were not able to unambiguously detect a core. Magnetic induction data indicates a small conducting core.

Lunar laser ranging (LLR) physical libration analysis shows that there is a liquid lunar core, first detected from dissipation at the core mantle boundary (CMB) and more recently from detection of CMB flattening and core moment of inertia. The core moment would correspond to a 390 km radius core if the core density is like iron, or larger if it has lower density or if an inner core exists. The core moment is the most important new lunar science result to come out of LLR. The tidal Love numbers are sensitive to internal elastic properties and structure including a core. At present, the LLR determination of the displacement Love number h_2 is compatible with the foregoing core size, but the k_2 Love number would work better with a smaller core. Future lunar range data should improve the uncertainties of the core moment and Love numbers.

Future LLR data should also greatly improve the determination of the CMB flattening which, like the core moment, is a recent detection that needs improvement. Low tidal Qs may result from a partial melt just above the CMB. A better determination of tidal Q vs frequency would be valuable.

Two of the free libration modes have big amplitudes. Future range data should also give insight into the cause of the free librations. The finite free librations require stimulation, but was that stimulation in the past or is it ongoing and possibly observable? Free librations show that the Moon has some activity affecting the dynamics.

LLR also contributes to orbit evolution. The mean motion and eccentricity changes are observed. While the mean motion and semimajor axis rates are compatible with our understanding of dissipation in Earth and Moon, LLR solutions consistently find an anomalous eccentricity rate. The anomalous eccentricity rate is a puzzle that needs to be solved, both for physical understanding and computation of dynamical evolution.

Three years of very accurate ranges from Apache Point Observatory show that our software is not fitting modern ranges to the subcentimeter level when the entire four decades of data are processed. Physical libration signatures were first seen in the postfit OCA residuals and they are clearly visible in the Apache Point residuals. The long-period excess of the residual spectra, discussed under the search for an inner core, could be due to the model or it could imply new science. Our physical models and analysis programs need to be improved to advance the science.

Ranging to the Apollo and Lunokhod retroreflecting arrays has provided a four-decades-long data set that has benefitted several science disciplines. Range accuracies have improved by two orders of magnitude since the Apollo era. The existing arrays spread laser pulses and may be contaminated with dust. A new set of widely distributed retroreflectors would be welcome, as would the recovery of Lunokhod 1. New devices should minimize the pulse spread and should be capable of operating in daylight with minimum thermal degradation of signal strength. A wider geographical distribution than the current pattern (Fig. 2) would increase sensitivity to physical librations and tides. There might be new lunar landers with corner cubes and other geophysical instruments by the middle of the coming decade.

Continued LLR data, improved software and new retroreflectors may open up new science possibilities while improving uncertainties for current solution parameters. New possibilities include the search for an inner core and seeking causes for the free librations. Attention has turned back to the Moon decades after the Apollo era missions. The current set of lunar orbiting spacecraft will be followed by new lunar landers, and that will offer opportunities for new ranging sites and accurate laser ranging for years to come.

Acknowledgments

References

Araki, H., S. Tazawa, H. Noda, Y. Ishihara, S. Goossens, S. Sasaki, N. Kawano, I. Kamiya, H. Otake, J. Oberst, and C. Shum, Lunar global shape and polar topography derived from Kaguya-LALT laser altimetry, *Science, 323*, 897-900, 2009.

Bills, B. G., and R. D. Ray, Lunar orbital evolution: a synthesis of recent results, *Geophys. Res. Lett., 26,* 3045-3048, 1999.

Brett, R., A lunar core of Fe-Ni-S, *Geochim. Cosmochim. Acta, 37*, 165-170, 1973.

Brett, R., and P. M. Bell, Melting relations in the Fe-rich portion of the system Fe-FeS at 30 kb pressure, *Earth and Planetary Sci. Lett., 6*, 479-482, 1969.

Calame, O., Determination des librations libres de la Lune, de l'analyse des mesures de distances par laser, *C. R. Acad. Sc. Paris, 282*, *Serie B*, 133-135, 1976a.

Calame, O., Free librations of the Moon determined by an analysis of laser range measurements, *The Moon, 15*, 343-352, 1976b.

Chapront, J., M. Chapront-Touzé, and G. Francou, Complements to Moons' lunar libration theory. Comparisons and fits to JPL numerical integrations, *Celestial Mechanics and Dynamical Astronomy, 73*, 317-328, 1999.

Chapront, J., M. Chapront-Touzé, and G. Francou, A new determination of lunar orbital parameters, precession constant and tidal acceleration from LLR measurements, *Astron. and Astrophys., 387*, 700-709, doi:10.1051/0004-6361:20020420, 2002.

Cisowski, S. M., D. W. Collinson, S. K. Runcorn, A. Stephenson, and M. Fuller, A review of lunar paleointensity data and implications for the origin of lunar magnetism, in *Proc. of the 13th Lunar and Planetary Sci. Conf.*, *J. Geophys. Res., 88*, A691-A704, 1983.

Cisowski, S. M., and M. Fuller, Lunar paleointensities via the IRMs normalization method and the early magnetic history of the Moon, in *Origin of the Moon*, edited by W. K. Hartmann, R. J. Phillips, and G. J. Taylor, pp. 411-424, Lunar and Planetary Institute, Houston, 1986.

Collinson, D. W., On the existence of magnetic fields on the Moon between 3.6 Ga ago and the present, *Physics of the Earth and Planetary Interiors, 34*, 102-116, 1984.

Dickey, J. O., P. L. Bender, J. E. Faller, X X Newhall, R. L. Ricklefs, J. G. Ries, P. J. Shelus, C. Veillet, A. L. Whipple, J. R. Wiant, J. G. Williams, and C. F. Yoder, Lunar laser ranging: a continuing legacy of the Apollo program, *Science, 265*, 482-490, 1994.

Eckhardt, D. H., Passing through resonance: The excitation and dissipation of the lunar free libration in longitude, *Celestial Mechanics and Dynamical Astronomy, 57*, 307-324, 1993.

Folkner, W. M., J. G. Williams, D. H. Boggs, The Planetary and Lunar Ephemeris DE 421, JPL IOM 343R-08-003, March 31, 2008.

Gagnepain-Beyneix, J., P. Lognonné, H. Chenet, D. Lombardi, and T. Spohn, Seismic model of the lunar mantle and constraints on temperature and mineralogy, *Physics of the Earth and Planetary Interiors*, *159*, 140-166, 2006.

Garrick-Bethell, I., B. P. Weiss, D. L. Shuster, and J. Buz, Early lunar magnetism, *Science, 323*, 356-359, 2009.

Goins, N. R., A. M. Dainty, and M. N. Toksoz, Lunar seismology: the internal structure of the Moon, *J. Geophys. Res.*, *86*, 5061-5074, 1981.

Goldstein, B. E., R. J. Phillips, and C. T. Russell, Magnetic permeability measurements and a lunar core, *Geophys. Res. Lett., 3*, 289-292, 1976.

Goossens, S. and K. Matsumoto, Lunar degree 2 potential Love number determination from satellite tracking data, *Geophys. Res. Lett., 35*, L02204, doi:10.1029/2007GL031960, 2008.

Gusev, A., N. Kawano, and N. Petrova, Fine phenomena of the lunar libration, abstract No. 1447 of *Lunar and Planetary Science Conference XXXVI*, 2005.

Hood, L. L., D. L. Mitchell, R. P. Lin, M. H. Acuna, and A. B. Binder, Initial measurements of the lunar induced magnetic dipole moment using Lunar Prospector magnetometer data, *Geophys. Res. Lett.*, *26*, 2327-2330, 1999.

Jolliff, B. L., M. A. Wieczorek, C. K. Shearer, and C. R. Neal, editors., New Views of the Moon, Reviews in Mineralogy and Geochemistry, vol. 60, The Mineralogy Society of America, Chantilly, VA, USA, 2006.

Jin, W., and J. Li, Determination of some physical parameters of the Moon with lunar laser ranging data, *Earth, Moon and Planets*, *73*, 259-265, 1996.

Khan, A., K. Mosegaard, and K. L. Rasmussen, A new seismic velocity model for the Moon from a Monte Carlo inversion of the Apollo lunar seismic data, *Geophys. Res. Lett., 27,* 1591-1594, 2000.

Konopliv, A. S., A. B. Binder, L. L. Hood, A. B. Kucinskas, W. L. Sjogren, and J. G. Williams, Improved gravity field of the Moon from Lunar Prospector, *Science 281*, 1476-1480, 1998.

Konopliv, A. S., S. W. Asmar, E. Carranza, W. L. Sjogren, and D. N. Yuan, Recent gravity models as a result of the lunar prospector mission, *Icarus, 150*, 1-18, 2001.

Konopliv, A. S., the LP150Q lunar gravity field is available on the PDS website http://pds-geosciences.wustl.edu/geo/lp-l-rss-5-gravity-v1/lp_1001/sha/jgl150q1.lbl

Kuskov, O. L., and V. A. Kronrod, Constitution of the Moon 5. Constraints on composition, density, temperature, and radius of a core, *Physics of the Earth and Planetary Interiors, 107*, 285-306, 1998.

Langseth, M. G., S. J. Keihm, and K. Peters, Revised lunar heat-flow values, in *Proc. Lunar Sci. Conf. 7th*, Pergamon Press, pp. 3143-3171, 1976.

Lognonné, P., J. Gagnepain-Beyneix, and H. Chenet, A new seismic model of the Moon: implications for structure, thermal evolution and formation of the Moon, *Earth and Planetary Science Lett.*, *211*, 27-44, 2003.

Lognonné, P., Planetary Seismology, Annual Reviews of Earth and Planetary Sci., 33, 19.1-19.34, doi: 10.1146/annurev.earth.33.092203.122604, 2005.

Lyard, F., F. Lefevre, T. Letellier, and O. Francis, Modelling the global ocean tides: insights from FES2004, *Ocean Dynamics, 56*, 394-415, 2006.

McCarthy, D. D., G. Petit (eds.), IERS Conventions (2003), IERS Technical Note No. 32, 2003.

Murphy, T. W., E. G. Adelberger, J. B. R. Battat, C. D. Hoyle, R. L. McMillan, E. L. Michelsen, C. W. Stubbs, and H. E. Swanson, APOLLO: One-millimeter Lunar Laser Ranging, in proceedings of 16th International Workshop on Laser Ranging, Poznan, Poland, Oct 13-17, 2008, 2009.

Nakamura, Y., Seismic velocity structure of the lunar mantle, *J. Geophys. Res.*, *88*, 677-686, 1983.

Nakamura, Y., Far deep moonquakes and deep interior of the Moon, *J. Geophys. Res., 110,* E01001, doi:10.1029/2004JE002332, 2005.

Newhall, X X, and J. G. Williams, Estimation of the lunar physical librations, *Celestial Mechanics and Dynamical Astronomy*, *66*, 21-30, 1997.

Pearlman, M. R., J. J. Degnan, and J. M. Bosworth, The International Laser Ranging Service, in *Advances in Space Research, 30 (#2)*, pp 135-143, doi:10.1016/S0273-1177(02)00277-6, 2002.

Petrova, N., and A. Gusev, Modeling of the free lunar libration, abstract No. 1448 of *Lunar and Planetary Science Conference XXXVI*, 2005.

Ping, J. S., Q. Huang, J. G. Yan, J. F. Cao, G. S. Tang, and R. Shu, Lunar topographic model CLTM-s01 from Chang'E-1 laser altimeter, submitted, 2008.

Ray, R., http://bowie.gsfc.nasa.gov/ggfc/tides/harm_fes04.html, 2007.

Rambaux, N., and J. G. Williams, A new determination of the normal modes of the Moon's libration, abstract for Division on Dynamical Astronomy meeting, Virginia Beach, VA, May 2-5, 2009a.

Rambaux, N., and J. G. Williams, The Moon's physical librations and determination of the free librations, in preparation, 2009b.

Righter, K., and M. J. Drake, Core formation in Earth's Moon, Mars, and Vesta, *Icarus*, *124*, 513-529, 1996.

Russell, C. T., P. J. Coleman Jr., and B. E. Goldstein, Measurements of the lunar induced magnetic moment in the geomagnetic tail: Evidence for a lunar core?, in *Proc. Lunar Planetary Science Conf. 12th*, pp. 831-836, 1981.

Schultz, P. H., M. I. Staid, and C. M. Pieters, Lunar activity from recent gas release, *Nature*, *444*, 184-186, doi: 10.1038/nature05303, 2006.

Sellers, P. C., Seismic evidence for a low-velocity lunar core, *J. Geophys. Res. Planets, 97,* 11663-11672, 1992.

Smith, D. E., M. T. Zuber, G. A. Neumann, and F. G. Lemoine, Topography of the Moon from the Clementine lidar, *J. Geophys. Res., 102,* 1591-1611, 1997.

Spohn, T., W. Konrad, D. Breuer, and R. Ziethe, The longevity of lunar volcanism: implications of thermal evolution calculations with 2D and 3D mantle convection models, *Icarus*, *149*, 54-65, 2001.

Stooke, P. J., Lunar laser ranging and the location of Lunokhod 1, abstract #1194, *Lunar and Planetary Science Conference XXXVI*, 2005.

Stooke, P. J., The International Atlas of Lunar Exploration, Cambridge University Press, New York, 2007.

Warren, P. H., and K. L. Rasmussen, Megaregolith insulation, internal temperatures, and bulk Uranium content of the Moon, *J. Geophys. Res.*, *92*, 3453-3465, 1987.

Williams, J. G., X X Newhall, and J. O. Dickey, Lunar Moments, Tides, Orientation, and Coordinate Frames, *Planetary and Space Science, 44*, 1077-1080, 1996.

Williams, J. G., D. H. Boggs, C. F. Yoder, J. T. Ratcliff, and J. O. Dickey, Lunar rotational dissipation in solid body and molten core, *J. Geophys. Res. Planets*, *106*, 27933-27968, 2001.

Williams, J. G., and J. O. Dickey, Lunar Geophysics, Geodesy, and Dynamics, Proceedings of 13th International Workshop on Laser Ranging, October 7-11, 2002, Washington, D. C., eds. R. Noomen, S. Klosko, C. Noll, and M. Pearlman, NASA/CP-2003-212248, pp. 75-86, 2003. http://cddisa.gsfc.nasa.gov/lw13/lw_proceedings.html

Williams, J. G., S. G. Turyshev, D. H. Boggs, and J. T. Ratcliff, Lunar Laser Ranging Science: Gravitational Physics and Lunar Interior and Geodesy, in *Advances in Space Research, vol. 37, Issue 1*, The Moon and Near-Earth Objects, 67-71, doi: 10.1016/j.asr.2005.05.13, 2006. [arXiv:gr-qc/0412049]

Williams, J. G., A Scheme for Lunar Inner Core Detection, *Geophysical Research Letters*, *34*, L03202, doi:10.1029/2006GL028185, (Feb 9) 2007.

Williams, J. G., D. H. Boggs and W. M. Folkner, DE421 Lunar Orbit, Physical Librations, and Surface Coordinates, JPL IOM 335-JW,DB,WF-20080314-001, March 14, 2008.

Yoder, C. F., The free librations of a dissipative Moon, *Philos. Trans. R. Soc. London Ser. A*, *303*, 327-338, 1981.

Yoder, C. F., Venus' free obliquity, *Icarus, 117,* 250-286, 1995.